RECENT ADVANCES IN LEAD–ACID CELL RESEARCH AND DEVELOPMENT*

ERNST VOSS

VARTA Batterie AG, Forschungs- und Entwicklungszentrum, Gundelhardtstr. 72, D-6233 Kelkheim/Taunus (F.R.G.)

Summary

The lead–acid battery is, and will be for the foreseeable future, the most widely used secondary energy storage system. It will maintain this predominant rôle because of its highly developed technology, its low cost as compared with other secondary systems, and its high reliability.

During the last decade it has been demonstrated that the lead–acid system is able to provide an attractive energy source of sufficient energy and power per unit weight and volume for its successful application to electric vehicle propulsion. Worldwide basic research has contributed to the improvement of both active material utilization and cycle life. This will be shown by a number of typical examples, such as the relations between active material properties and capacity at high rates of discharge, the effect of acid stratification, and others. Simultaneously, the expenditure on the maintenance of lead–acid batteries has been minimized by the development of peripheric equipment such as recombination devices and means for central-automatic water refill. It will be shown that there is still a considerable potential for further improvement which might further strengthen the unique position of the lead–acid system in the market by comparison with competitive systems.

1. Introduction

If the last two decades of lead–acid cell research and development are reviewed, it can be stated that a remarkably great improvement in energy density and power density has been achieved: properties which are of particular importance for the application of lead–acid batteries for electric vehicle propulsion. As will be immediately evident to the reviewer, these achievements must be attributed to the effort spent on electrochemically inert components such as grids and top lead, separators and jar materials. Almost

*Paper presented at the NERDDC Workshop on Power Sources for Electric Vehicles, Adelaide, August 23 - 25, 1980.

0378-7753/82/0000-0000/$02.75 © Elsevier Sequoia/Printed in The Netherlands

no progress has been made in respect of active material utilization and cycle life.

Although electrochemists have made important contributions to the basic understanding of the lead–acid cell the work on modelling of electrodes and cells in the industry is still performed on a more or less empirical basis. It is well known, however, that an evolutionary process of improving cell behaviour will become more and more difficult, expensive, and time-consuming, and progress in development will become smaller as the natural limit is approached. Mathematical modelling appears to be the most promising method to reduce costs and to meet the development goals reliably. Battery engineers have recognized this fact and increasingly are calling upon the electrochemists to prove the value and validity of their theories for practical application. In view of the complexity of the problem and the lack of practicable quantitative relationships in most cases this, indeed, is not an easy task.

There is no doubt that the active material utilization and the cycle life of an electrode are dependent on the properties or "internal parameters" of the active materials themselves, as well as on the "external parameters" which are imposed on the cell, such as current density, temperature, etc.

On the other hand, the internal parameters are largely determined by the "production parameters". The relations between these three sets of parameters are qualitatively shown in Fig. 1. It can be seen that the surface area of the positive active material, for example, is influenced by the PbO content of the initial lead oxide, but as we know from experience, to a

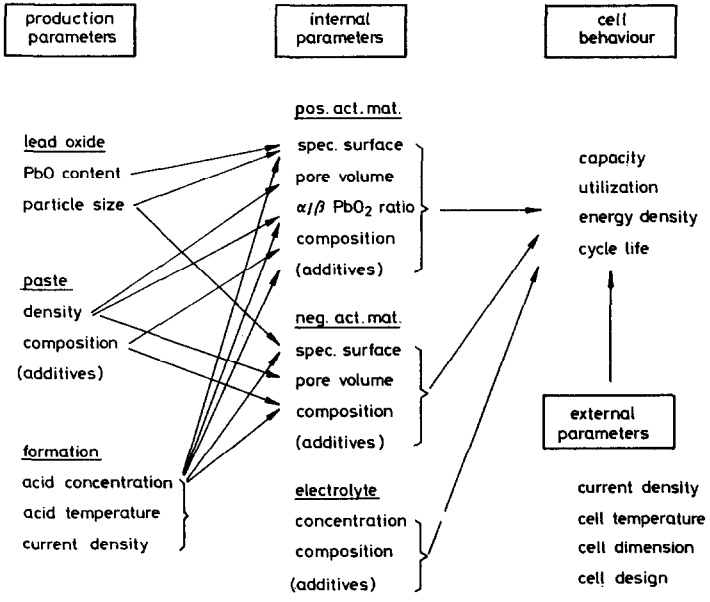

Fig. 1. Relationship between production parameters, internal parameters, external parameters and cell behaviour.

much greater extent by the formation conditions, whereas the pore volume of the positive as well as of the negative active material is determined by the density of the paste. Cell behaviour, however, is not only determined by the internal parameters. As is well known, external parameters such as current density, cell temperature, and cell design, have a strong influence.

At the present time it must be said that no quantitative relation between production parameters and internal parameters has been developed. In this field we must rely entirely upon empirical knowledge. In recent years, however, such relationships between internal and external parameters on the one hand, and cell behaviour on the other, have been established. It is the purpose of this paper to show by way of some examples how successful these attempts have been and the limitations that still exist.

Further important contributions to the lead–acid cell, especially with regard to its application to electric vehicles and load leveling, have been made in the field of maintenance. The steps that have been taken to achieve an almost maintenance-free battery operation will be briefly pointed out.

2. The relation between internal parameters and electrode capacity at high rates of discharge and temperatures below 0 °C

High rates of discharge at low temperatures are not only primarily of importance for SLI batteries but also for electric vehicle batteries. For SLI batteries the so-called low temperature cranking capability has been included in US and European industrial specifications. So far no low temperature specification is known for electric vehicle batteries. However, it is evident that low temperature discharge problems might occur. Therefore, the behaviour of the lead–acid cell under these conditions is of particular interest.

2.1. Theoretical considerations

The basis of the theoretical considerations is the theory of porous electrodes as developed by Winsel [1 - 3]. The pore model used by him is preferred, since it appears to be more accurate for the description of a porous electrode than the continuum model. As was shown by Wendtland [4] the continuum model can be replaced by a pore model having cylindrical pores of constant diameter and *vice versa*. It is further assumed that the formation of a passivating layer of $PbSO_4$ during discharge occurs *via* a solution/precipitation mechanism in accordance with Vetter [5], and from this it is quickly evident that the diffusion of $PbSO_4$ (Pb^{2+}) species away from the electrode surface through the $PbSO_4$ diaphragm is one rate and capacity determining process during discharge. The thickness of this diaphragm increases during discharge to such an extent that finally, due to a high supersaturation at the surface, spontaneous precipitation of $PbSO_4$ occurs, thus producing a rapid voltage decay which indicates the end of discharge.

If we make a calculation on the basis of this model (the exact procedure for which has been published earlier [6]) we obtain the following relationship:

$$It^* = \frac{1}{\Delta V_0}\left\{\left[S - \int_0^{r_t^*} 0(r)\mathrm{d}r\right]\frac{r_t^*}{2} + \int_0^{r_t^*} V(r)\mathrm{d}r\right\}. \quad (1)$$

Assuming that the current producing lead surface does not change very much and further assuming that there is no microporosity in the negative active material, we finish with the following simple capacity equation:

$$C_{HS} = K\frac{S^2}{I} \quad (2)$$

$$K = \frac{FP^2D\Delta c}{\lambda \Delta V_0}.$$

(P = porosity, λ = tortuosity factor of the $PbSO_4$ diaphragm, Δc = supersaturation concentration of $PbSO_4$, ΔV_0 = volume change of active material, F = Faraday constant, D = diffusion coefficient, and S = surface area of active material.)

As can be seen, the capacity, especially at high rates, is proportional to the second power of the surface area of the active material and inversely proportional to the current. This equation can easily be checked experimentally, as will be shown later.

Lead sulphate passivation — as we may call this type of capacity limiting process for short — can only occur as long as sufficient acid is made available either in the pores of the active material or by diffusion or convection (or forced flow) from outside. If this is not the case, the capacity is determined by the amount of electrolyte or limited by electrolyte deficiency. Under these conditions the capacity is given by eqn. (3):

$$C_{HV} = 2\kappa F V_p \Delta m. \quad (3)$$

(V_p = pore volume of active material, Δm = available amount of acid per volume of initial electrolyte, κ is a factor close to 1, which takes into account transference and diffusion of H_2SO_4 from outside the porous system.)

What happens at temperatures below 0 °C? If we discharge, for instance, at −18 °C (a temperature which is used in most specifications) we dilute the electrolyte within the porous system. As is obvious from Fig. 2, showing the lower end of the H_2SO_4/H_2O phase diagram, we move from point y_0 to point y^1 on the liquidus curve. As soon as we proceed further ice crystals are formed which are deposited on the lead surface as a diaphragm showing exactly the same effect as the $PbSO_4$ diaphragm mentioned earlier. Therefore, we call this process ice passivation.

It is evident that at a certain specific point depending on the internal parameters, $PbSO_4$ passivation should change over to ice passivation and *vice versa*. At this point C_{HS} and C_{HV} are expected to be equal: $C_{HV} = C_{HS}$.

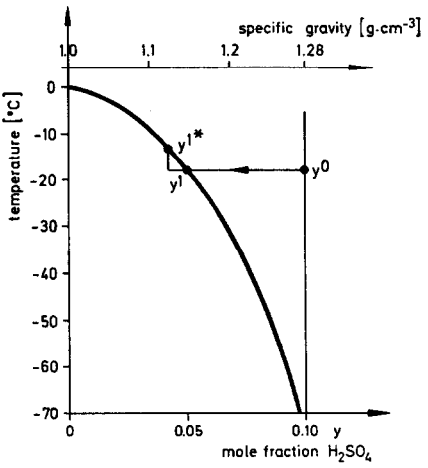

Fig. 2. Lower end section of the H_2SO_4/H_2O phase diagram.

By substituting and rearranging the equation $C_{HS} = C_{HV}$ we obtain a critical factor f^*:

$$f^* = \frac{V_p}{S^2}. \tag{4}$$

Once we have determined f^* experimentally we are in a position to decide, from simple measurements of the two internal parameters V_p and S of the active material, whether $PbSO_4$ or ice passivation will take place at a given temperature, electrolyte concentration, and current density.

2.2. Results and discussion

From further consideration of eqn. (3) it will become evident that by investigating the capacity C_H of a series of electrodes having identical internal parameters in dependence of Δm, *i.e.*, in dependence of the acid concentration, a point should be found where $C_{HV} = C_{HS}$. This would give us the necessary data to calculate the critical factor f^*.

Figure 3 shows the results which have been obtained by such an investigation . In the Figure the capacities of both negative and positive electrodes obtained at −18 °C and ~150 mA/cm² are plotted *versus* the acid concentration. As can be seen, both curves meet the concentration axis at the same point, namely 2.25 mole/l or $x = 0.042$. This indicates that for both electrodes at least the limiting process must be the same. The curve for the negative electrodes exhibits a maximum at 4.50 mole/l. This is obviously the transition point where $C_{HV} = C_{HS}$, *i.e.*, where the $PbSO_4$ passivation changes to ice passivation and *vice versa.*

From the data of this point the critical factor f^* is calculated to be 0.73×10^{-8} g cm^{-1}.

On the left hand side we have ice passivation and on the right hand side we must expect $PbSO_4$ passivation. At very high acid concentrations

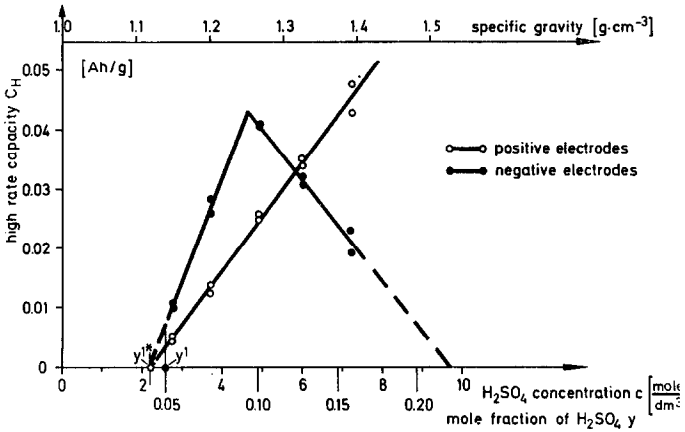

Fig. 3. High rate capacity of positive and negative electrodes (−18 °C) as a function of electrolyte concentration.

of about 9 - 10 mole/l the electrode capacity is again 0. In this range of acid concentration the $PbSO_4$ solubility attains a minimum. We assume that this is related to the particular behaviour of negative electrode capacity. More detailed investigation is necessary.

On further examination of the curve for the positive electrodes in Fig. 3 it will become evident that there is no $PbSO_4$ passivation at all. In the acid concentration range investigated we observed ice passivation only. This is due to the high specific surface area of the positive active material, which is about 10 times higher than that of the negative active material. This result is supported by another experiment.

The slope of the positive curve being different from that of the negative curve expresses the fact that water is formed in addition to $PbSO_4$ on the positive electrode, and the transfer of HSO_4^- ions is away from the electrode, whereas at the negative electrode there is a transfer of HSO_4^- ions onto the electrode.

As we have learned from eqn. (2), the capacity of an electrode should be proportional to S^2 as long as $PbSO_4$ passivation occurs. To check this relationship we have prepared a series of electrodes having different specific surface areas but constant pore volume. The results of capacity measurements on these electrodes (again at −18 °C and i = 150 mA/cm^2) are given in Fig. 4.

As can be seen, most of the experimental points fit quite well to the curve (solid line) calculated from eqn. (2). A group of points, however, shows considerably lower capacity than expected. A detailed analysis of these points shows that eqn. (2) is not valid for these electrodes because there was no $PbSO_4$ passivation, but ice passivation had occurred. If we take, for instance, the characteristic values of the point (marked by a circle) which is lying on the borderline, and calculate a critical factor f^*, we obtain

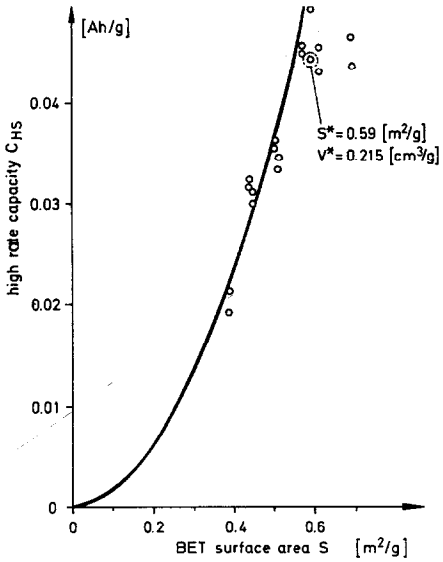

Fig. 4. High rate capacity (150 mA/cm^2) of negative electrodes obtained at −18 °C as a function of surface area of the negative active material. ——, calculated from eqn. (2); ○, experimental values.

$f^* = 0.62 \times 10^{-8}$ g cm^{-1} which is very close to the earlier f^* values obtained in a quite different and more exact way.

This again clearly shows that the electrodes represented by the group of deviating points have undergone ice passivation.

As we have learned earlier, positive electrodes normally show ice passivation only. If this is correct, no surface area effect of positive active material on the capacity should be expected. In Fig. 5 we have plotted capacity

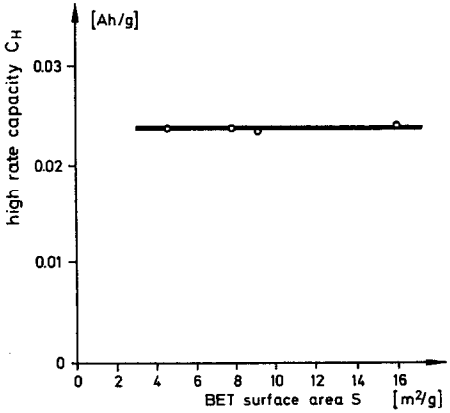

Fig. 5. High rate capacity of positive electrodes obtained at −18 °C as a function of surface area of positive active material.

data obtained on positive electrodes (−18 °C; 150 mA/cm^2) *vs.* BET surface of positive active material. As can be seen there is no effect of surface area at all. We know, however, from earlier measurements that the capacity of positive electrodes depends greatly on the pore volume of the positive active material, and this is in excellent agreement with the occurrence of ice passivation at positive electrodes.

In summarizing this section the following achievements of immediate practical importance can be stated. The qualitative understanding of the high rate, low temperature discharges now enables us:

— to detect and locate failures more easily than before in cases of insufficient capacity;

— to calculate the capacity of electrodes from data obtained by simple physical measurements (BET surface and pore volume) of some internal parameters;

— to design active materials for high rate, low temperature discharges and to calculate the correct active material balance in a cell;

— to produce such active materials by choosing and applying the adequate production parameters;

— to design and apply new processes which allow a closer control of the production parameters and consequently of the internal parameters.

3. The relation between internal parameters and electrode capacity at temperatures above.0 °C

At normal temperatures and at discharge rates of practical relevance (10 h - 0.1 h rate) the capacity of porous Pb (PbO_2) electrodes is generally determined by acid depletion ("water passivation"). If the discharge is performed under forced flow of electrolyte through the pores of the active material, $PbSO_4$ passivation is assumed to be the limiting process. As will be explained later, under this condition the $PbSO_4$ generated subsequently fills the pore volume. The effect of these two mechanisms on the active material utilization in dependence on the discharge current density is shown in Fig. 6. A third mechanism which is based on the degradation of electronically conducting paths in the active material must also be taken into consideration, especially at great depths of discharge.

The acid depletion mechanism implies that after the end of discharge and an intermittent rest period, the electrode can be repeatedly discharged to a certain extent due to the relaxation of the acid concentration, the relaxation time being of the order of 30 min. A relaxation and, consequently, a repeated discharge is impossible if the first discharge has been performed under forced flow conditions, *i.e.*, if $PbSO_4$ passivation has occurred.

3.1. Capacity determined by $PbSO_4$ passivation

The results presented in Fig. 6 show that under electrolyte forced flow a remarkable increase in the utilization of the negative active material is

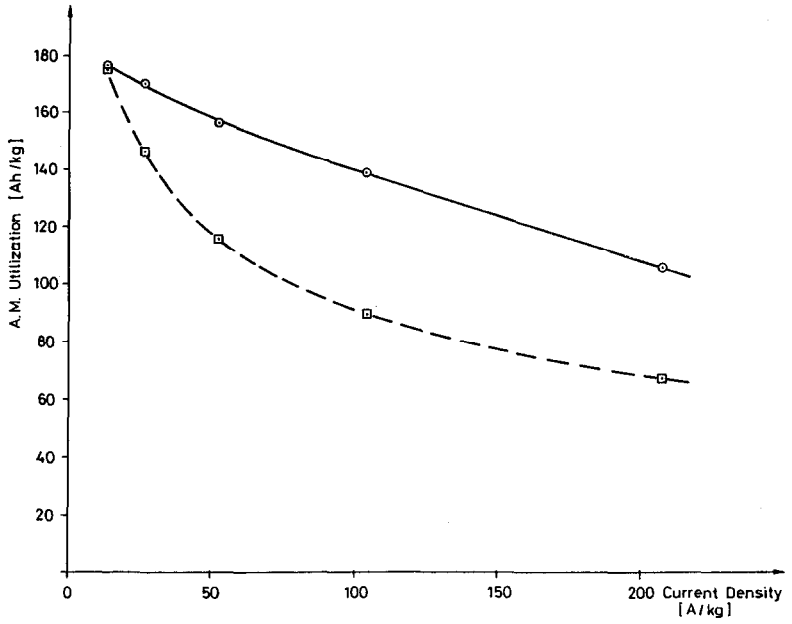

Fig. 6. Active material utilization of Pb electrodes as a function of discharge current density with (—⊙—) and without (- - -⊡- - -) forced flow of electrolyte. Acid concentration: 0.092 mole fraction.

observed over a wide range of discharge current densities. As compared with the non-forced flow condition the increase is especially high at about the one hour rate of discharge, which is of particular interest for electric vehicle batteries. At very low and very high rates of discharge the difference approaches zero. An explanation of this characteristic behaviour can be qualitatively derived from eqn. (1). The first term on the right hand side of this equation describes the effect of the internal surface area on the capacity, whereas the second term is related to the effect of the pore volume. Under forced flow conditions of discharge, at any rate applied in the experiment of Fig. 6, the pores are continuously filled with $PbSO_4$. Starting with the small pores and successively filling pores of increasing size the current producing surface area is reduced. This process is equivalent to an increase in current density which finally results in a voltage decay indicating the termination of discharge. It is evident that this occurs as soon as the surface of the coarse pores, which makes only a negligible contribution to the total surface area, is passivated by the mechanism of $PbSO_4$ passivation. Therefore, the utilization of the active material discharged under forced flow of electrolyte at rates lower than 400 A/kg does not depend on the surface area, *i.e.*, in eqn. (1) the first term on the right hand side can be neglected and the capacity is determined by the pore volume, as given by the second term of eqn. (1).

The same considerations are valid for discharges at very low rates under non-forced-flow conditions, and at infinitely small current densities the capacity is expected to be identical with the capacity obtained at very low rates under forced flow conditions. Indeed, if we extrapolate the results given in Fig. 6 to zero current density, we arrive at approximately 200 Ah/kg for both curves.

At very high rates of discharge we can again expect that both capacity values approach the same value, since under forced flow as well as under non-forced-flow conditions we shall observe the same passivation mechanism, namely, $PbSO_4$ passivation again, however, with no, or only a small number of small pores being entirely filled with $PbSO_4$.

Since this is a $PbSO_4$ surface passivation analogous to the mechanism observed under high rate, low temperature discharges (*cf.* Section 2), the capacity now depends on the surface area and may be calculated from eqn. (1) neglecting the second right hand term, or from eqn. (2) by analogy with the procedure outlined in Section 2 (low temperature, high rate discharge).

It would appear that eqn. (1) is of general importance, and at present we are collecting more experimental data to prove its validity over the total range of external parameters: current density, cell temperature, and acid concentration.

3.2. Capacity determined by acid depletion

As already pointed out, the capacity of lead–acid electrodes (under non-forced flow conditions) is normally determined by acid depletion (or "water passivation"). It is evident that a passivation mechanism of this kind must be subjected to a relaxation. As a consequence, an additional amount of capacity can be obtained from a discharged electrode after a certain rest period, as is well known. The effect of repeated discharges after a rest period of 30 min on the capacity of a negative electrode is shown in Fig. 7. Analogous results are obtained on positive electrodes.

It has been proposed recently [7] that repeated discharges with intermittent rest periods might be treated on the basis of a mathematical model generally valid for relaxation processes. On this basis, after some calculations (which will be published in detail elsewhere [8]) we obtained the following equation:

$$it_e + i\frac{\gamma}{\alpha}(1 - \exp(-\alpha t_e)) = 1 \qquad (5)$$

(i = current density, t_e = discharge time, γ = a term related to the pore volume, α = time constant).

The values for α and γ can be determined from the electrode thickness and pore volume. In addition, for the numerical calculations of eqn. (5), the capacity values obtained on the first discharge in dependence on the discharge current must be determined experimentally, *i.e.*, this is a semi-empirical treatment. In Fig. 7 the calculated values are represented by solid lines. As can be seen these curves adequately describe the experimental

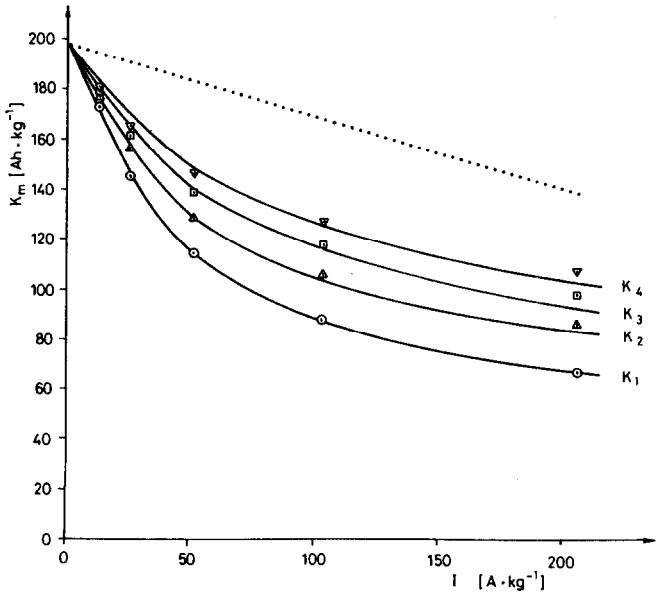

Fig. 7. Comparison of the calculated capacity function $K_m(I)$ of a Pb electrode without forced flow of electrolyte. Acid concentration y = 0.092.

behaviour of the system. The dotted curve represents the capacity which is obtained after infinite repetition of discharges with intermittent rest periods. This curve is in approximate accordance with the capacity curve obtained under forced flow.

In summarizing this section, it can be stated that a general mathematical relationship (eqn. (1)) has been derived between electrode capacity and the internal parameters of the active material under various conditions (external parameters). So far the electrode behaviour can be understood quantitatively at low temperatures and high rates of discharge. It is expected, however, that the validity of eqn. (1) will be extended to any rate and temperature.

It must be further stated that apart from some empirical relationships, no knowledge is available which allows for quantitative theoretical treatment of the cycle life. As a first approach to this problem the transformation laws are being studied [9], *i.e.*, the processes by which $PbSO_4$ is formed during discharge and Pb or PbO_2 is produced during charge, as well as the effect of these processes on the internal parameters of the active materials.

4. Peripheric equipment for lead–acid batteries

Apart from high power and high energy density the special application of lead–acid batteries to the propulsion of electric vehicles requires a long

cycle life and possibly maintenance-free operation. It will be shown by some examples the steps which have been taken to achieve these goals.

4.1. Water refilling

Maintenance of lead–acid batteries primarily consists of compensation for the water loss due to electrolytic water decomposition which mostly occurs during the overcharge period. Refilling of many cells with water is time consuming and costly. Therefore, battery engineers have developed several methods for automatic refilling or for the recombination of the hydrogen/oxygen gas being evolved from the cell. An automatic water refilling system is shown in Fig. 8. During the charging period the tube system on top of the battery is connected to a water reservoir. The amount of water necessary to attain the correct electrolyte level is controlled by a float gage, an example of which is shown in Fig. 9. The main disadvantage of an automatic water refilling system lies in the sensitive moving part of the float gage, which may lead to mechanical failures and uncontrolled water addition. This may be overcome by applying small pressure pulses to the system during refilling.

Recombination devices are free from moving parts and since they immediately remove hydrogen/oxygen as well as stibine from the cell they

Fig. 8. Battery with water refill system and central degassing.

simultaneously afford safety against explosions and noxious hazards. Recombination devices thus appear to be ideal means of considerably reducing the expense of maintenance and meeting safety requirements reliably. However, they have to be designed correctly, *i.e.*, their size and the arrangement of the various components must be adjusted to the cell and the acceptable overcharge current. The recombination rate can be nearly 100%. Recombination devices have been built and successfully tested in the range 5 - 430 W thermal power, which is equivalent to overcharge currents from about 3 A to about 290 A. A number of typical devices is shown in Fig. 10.

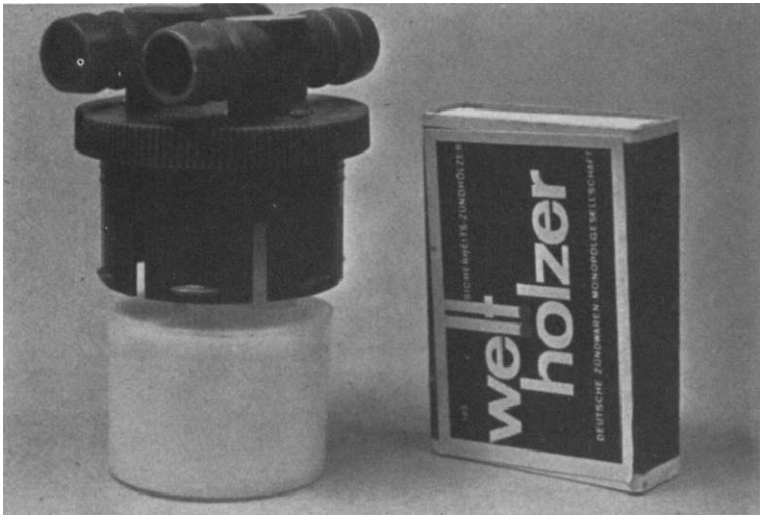

Fig. 9. Float gauge.

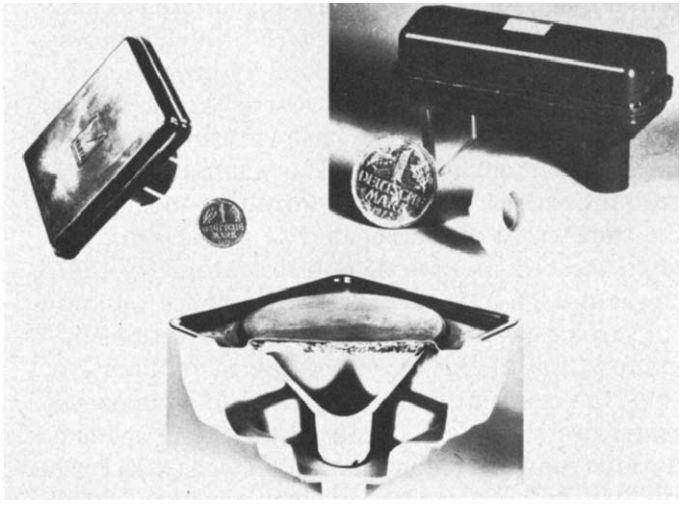

Fig. 10. Recombination devices (5 A, 10 A, 20 A).

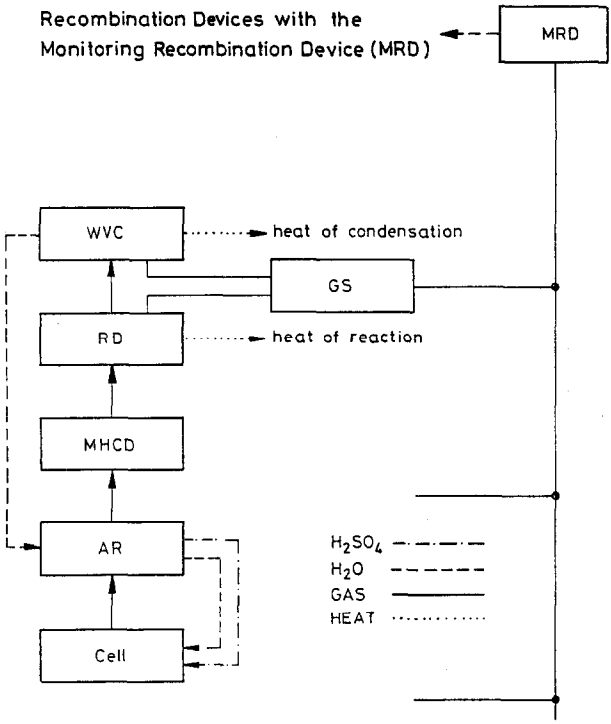

Fig. 11. Recombination devices with the monitoring recombination device (MRD).

The mathematical modelling of recombination devices is well known today. As can be seen from Fig. 11 a recombination device (RD) consists of components having the following functions: the hydrogen/oxygen mixture from the cell passes through the aerosol retainer (AR) which removes any H_2SO_4 from the gas. It then flows through the metal hydride decomposer (MHCD) which removes stibine and eventually arsine. At the catalyst (RD) the recombination to water takes place. The heat of reaction has to be transferred and dissipated to the environment. The water vapour is condensed at the water vapour condensor (WVC), from which the heat of condensation must also be transferred and dissipated to the environment and the water is returned to the cell. In case of non-stoichiometry the surplus gas is stored in the gas storage (GS). From our experience we know that only small amounts of surplus gas occur under normal conditions of operation. In case of a malfunction of the cell or of any recombination device component or even of the charger and its control system, an excess of gas may cause an overpressure in the gas storage (GS). Some gas may escape and flow to the so-called monitor recombination device (MRD) where the heat of recombination may be converted to an acoustic signal which draws attention to the malfunction.

If the recombination device is designed correctly, no overheating, even at overcharge currents much higher than the rated overcharge current, can occur. It is obvious that from 1.5 moles of a stoichiometric H_2/O_2 mixture we obtain 1 mol of water vapour.

From the gas law $pv = nRT$ it can be calculated that the relationship between the temperature of the catalyst T_2 and the gas temperature T_1 is given by: $T_2 = 1.5\ T_1$ under equilibrium conditions. A rise of catalyst temperature would produce a pressure rise which would decrease the flow of the H_2/O_2 mixture. Consequently, due to the reduced recombination rate, the catalyst temperature also decreases, thus providing a self-regulating control mechanism which, however, only works if there is no forced flow of the H_2/O_2 mixture through the catalyst substrate. For the efficiency of the recombination device the area of the catalyst substrate and the area of the water vapour condenser are critical. The mathematical modelling of this particular device has shown that 3.9 and 13.4 cm^2 of catalyst and water vapour condenser area are required, respectively, for each ampere of overcharge current [10].

The metal hydride decomposer (MHCD), on the other hand, determines the life of the device. The decomposition capacity of the MHCD is limited by its volume. For the type of MHCD used it has been found experimentally that a volume of approximately 8 ml is required per ampere of overcharge current. For large recombination devices it has been found to be of advantage to use exchangeable cartridges as MHCD. Thus the device can be used for more than 2000 cycles.

4.2. Acid stratification

Lead–acid batteries for electric road vehicle propulsion may have charge/discharge regimes which differ very much from those being applied to normal traction batteries. Fork lift trucks and other indoor vehicles are mostly operated on a shift basis. This generally provides sufficient time for a careful recharge of the battery, including an overcharge period, where gassing, because of its stirring effect, equalizes the acid concentration. In a battery powered bus line which has been in operation for many years in Germany this was not possible. An equalizing charge of the batteries was made only weekly. The batteries showed premature failure after about 800 cycles. Sulfation at the bottom of the negative plates had occurred which could be attributed to acid stratification.

As shown by Winsel [11], acid stratification develops in a lead–acid cell during charge and discharge because the density difference of the acid in the pores and in the free electrolyte between the plates results in a flow of high density acid to the bottom of the cell (*cf.* Fig. 12). As a consequence a stable acid stratification is generated in the gravitational field of the earth. A non-uniform current distribution and active material utilization will result which finally affects the cycle life. The relaxation of the stratification, *i.e.*, the equalization of the acid concentration, requires considerable time because of the low osmotic transport and diffusion rate. Gassing or purposive mixing

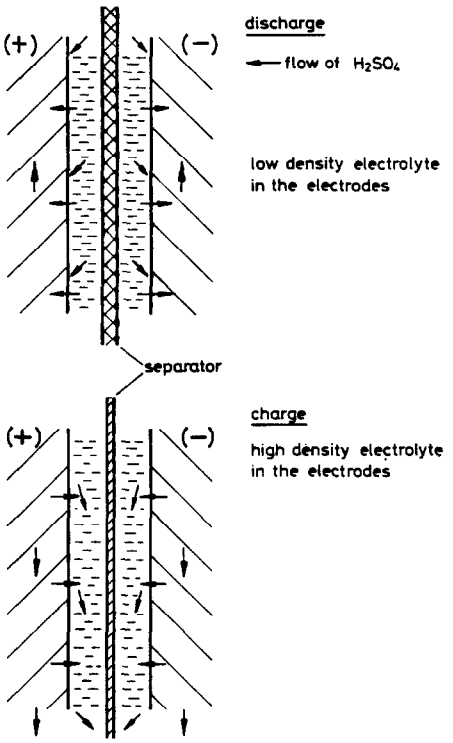

Fig. 12. Development of acid stratification.

of electrolyte increases the rate. Gassing due to overcharge, however, is disadvantageous for a cell, especially if it is extended over several hours. During overcharge at the elevated oxygen overpotential the corrosion rate of the positive grid as well as the shedding rate of the active material are higher than normal. Stirring or mixing of the electrolyte would improve the situation without these detrimental side-effects.

Furthermore, if extensive overcharging can be reliably avoided, the overall energy efficiency of a lead–acid battery is considerably improved. In summary, by stirring the electrolyte we achieve a low corrosion and shedding rate and, therefore, a longer cycle life, and the highest possible energy efficiency, because almost no overcharge is necessary.

Electric vehicle batteries with provisions for electrolyte stirring are being field tested at the present time. The electrolyte is stirred by an air lift pump which is inserted into each cell beside the plates. The pump consists of a thin sheet of plastic with a number of small tubes; the design can be seen from Fig. 13. Pressurized air is used for its operation. After charge a period of about 10 min is sufficient to obtain an electrolyte of uniform density again. The effect of stirring is shown in Fig. 14. In this experiment the acid density was determined over the plates of two cells, one with and the other without a pump. It is evident that after the first recharge acid stratifica-

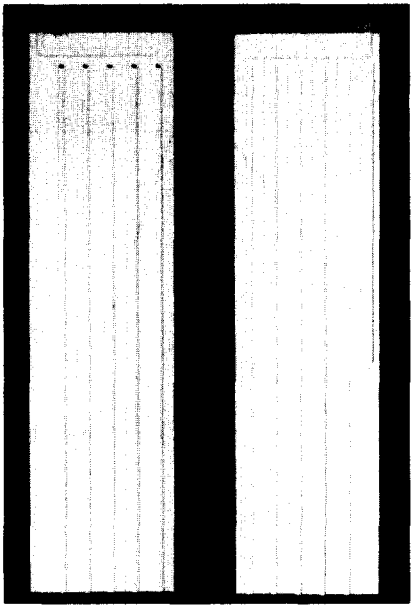

Fig. 13. Water air-lift pump.

tion has already occurred this state will be maintained for many cycles if there is no stirring effect such as gassing or the use of a pump (dashed line). However, if the acid is being circulated by use of the air lift pump for a short period only, the original acid density is obtained, indicating that the electrolyte concentration is again uniform.

From the considerations given above it may be expected that cells with electrolyte circulation will exhibit a cycle life longer than those without circulation provided that there is a small amount of overcharge only. This, indeed, has been found on a bench test as can be seen from Fig. 15.

In this experiment it was also found that the water loss was reduced considerably due to the low overcharge. Remembering the considerations concerning recombination devices, we now have the possibility of reducing their size for the same reason, if a recombination device is employed in addition to an air lift pump. Since there is a significant increase in cycle life, analogous results can also be expected from the field test. Acid circulation and its beneficial effect on the life of a lead–acid cell and on the energy efficiency results in an improvement in the economics of the electric vehicle.

Because acid circulation maintains the uniformity of the acid concentration, the uniformity of the current density distribution during discharge and charge is also maintained. Therefore, it can be concluded that the utilization of the active material during discharge, and the charge acceptance during charge, will also be improved. This has been shown in a model experiment [12] the principle of which is schematically shown in Fig. 16. The acid stratification can be simulated by a number of cells, *e.g.*, two cells in

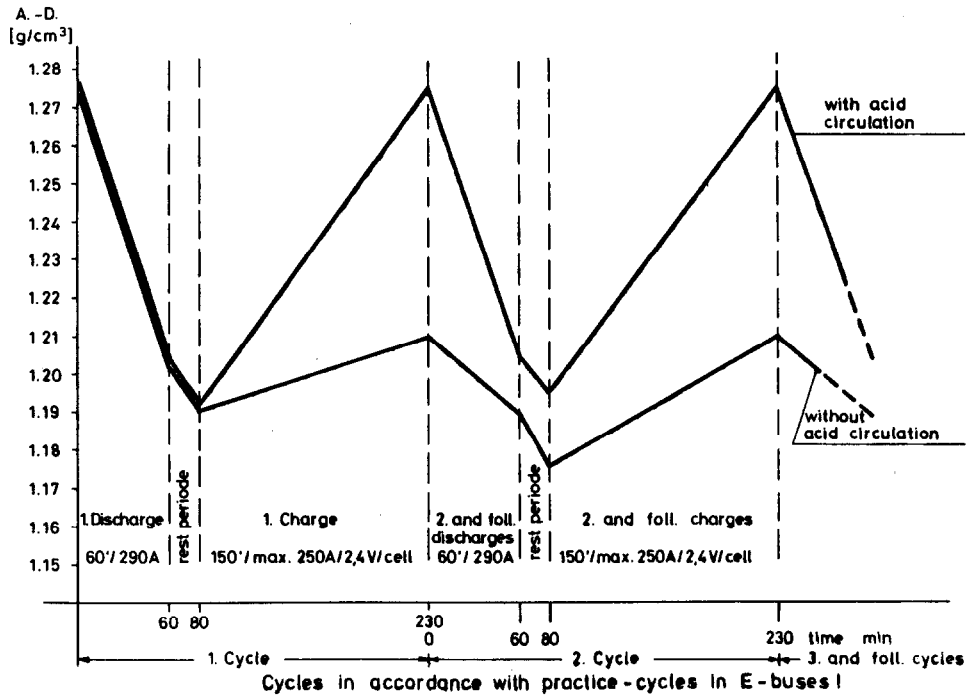

Fig. 14. Acid density during cycling.

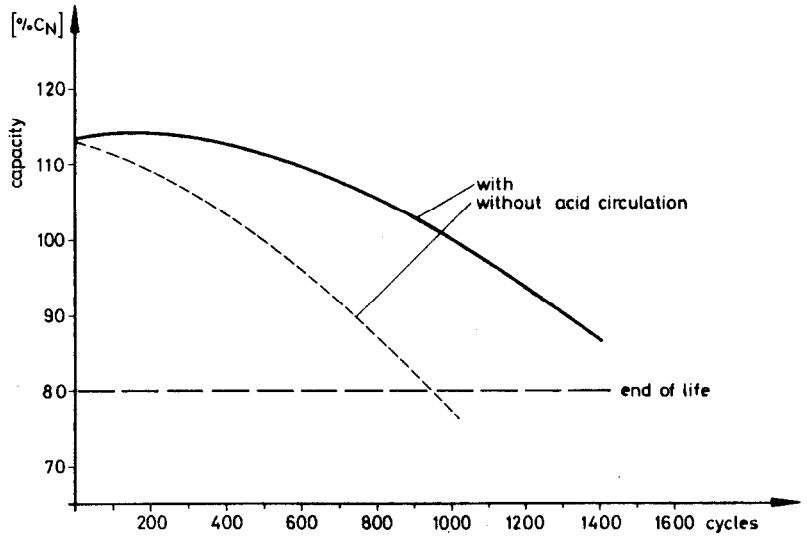

Fig. 15. Cycle life of traction cells type 7 PzF 455 with, and without acid circulation.

Fig. 16, connected in parallel and filled with acid of different gravities. The currents I_1, I_2, etc., in each cell can be easily measured and related to the total current I_g. The results obtained in this experiment at two different

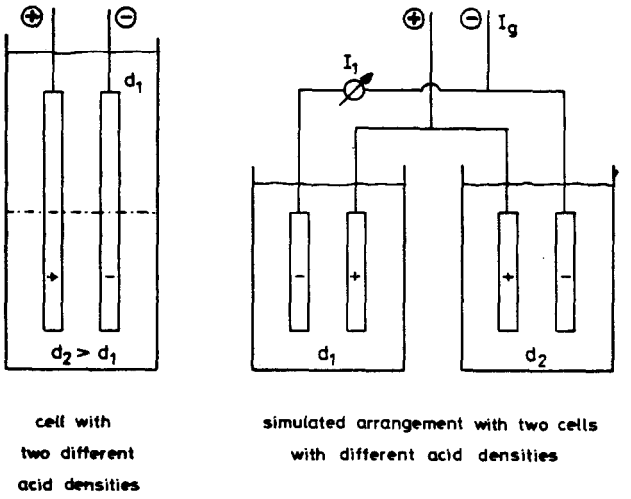

Fig. 16. Model experiment: current distribution under acid stratification conditions.

densities, $d_1 = 1.15$ g/cm^3 and $d_2 = 1.33$ g/cm^3, are summarized in Fig. 17 and compared with those which have been obtained when $d_1 = d_2 = 1.24$ g/cm^3. In the latter case we find, in agreement with expectation, a uniform current distribution and a capacity on discharge higher than that obtained

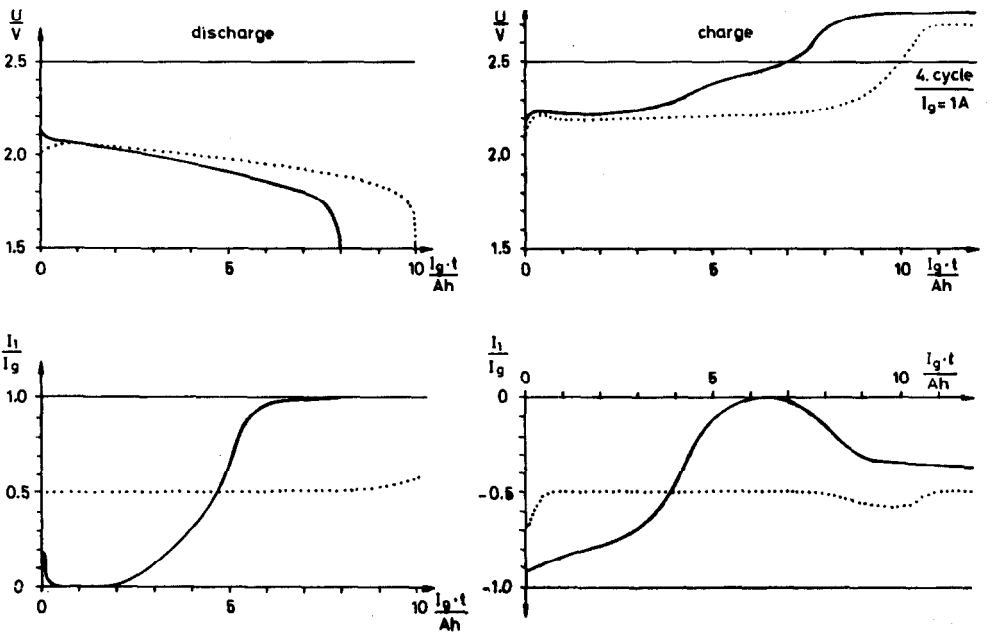

Fig. 17. Voltage and current distribution of the cell arrangement given in Fig. 16 at discharge and charge, constant total current $I_g = 1$ A. Solid line, $d_2 > d_1$; dotted line, $d_2 = d_1$.

with acid stratification ($d_1 < d_2$). On recharge we again observe a more uniform current distribution when $d_1 = d_2$ and, simultaneously, a better charge acceptance as indicated by the voltage curve.

5. Conclusions

After a period of successful development of lead–acid batteries of high energy and power density for electric vehicle propulsion which has been devoted almost entirely to the minimization of the weight of inactive components, there still exists free scope for further improvement. As concerns the inert components, partial replacement of grid lead by plastic material or the new through-the-partition connection, as recently proposed in Australia, may be mentioned.

It is evident, however, that there is a very high potential for the improvement of active material utilization, especially in the range of discharge rates which is of particular interest to electric vehicle application, if forced flow of electrolyte is applied. This method is also of importance from a more basic point of view. As pointed out, the application of forced electrolyte flow provides — in combination with other information — a useful tool to discriminate between different passivation mechanisms. From the data obtained in this way the derivation of quantitative relationships between electrode capacity and internal and external electrode and cell parameters can be expected, which hopefully may be useful for mathematical modelling of cells in the lead–acid industry.

So far as production parameters are concerned, our present knowledge of their effect on internal electrode parameters is rather empirical. Mathematical treatment of the formation, which determines the transformation laws of this process, is still very rudimentary. The same is true for the transformation laws of the cycle life determining processes. Nevertheless, it seems obvious that a further improvement in battery life is possible even under the conditions prevailing in electric vehicle applications.

In the future the lead–acid battery for electric vehicle propulsion will no longer be a simple battery. In connection with various peripheric equipment it will be a self-controlling and self-regulating power source, in other words, a system of high reliability and safety and low maintenance expenditure. This undoubtedly will also affect other application areas of the lead–acid battery.

Acknowledgements

Part of this work was supported by the US Department of Energy under Contract ANL 31-109-38-4438, the International Lead Zinc Research Organization under Contract LE-277, and the Bundesministerium für Forschung und Technologie under Contract ET 4046-B.

The author is indebted to his colleagues Prof. Dr A. Winsel, Dr W. Kappus, Dr K. Ledjeff, Dr J. Schulz and U. Hullmeine for their help and assistance.

References

1 A. Winsel, *Dissertation*, T.H., Braunschweig, 1957.
2 A. Winsel, *Z. Elektrochem.*, *66* (1962) 287.
3 A. Winsel, *Adv. Energy Convers.*, *3* (1963) 677.
4 R. Wendtland, *Diplom-Arbeit*, T.H., Braunschweig, 1963.
5 K. J. Vetter, *Chem.-Ing.-Tech.*, *45* (1973) 213.
6 A. Winsel, U. Hullmeine and E. Voss, *J. Power Sources*, *2* (1977/78) 369.
7 U. Hullmeine, W. Kappus, J. Schulz, E. Voss and A. Winsel, *ILZRO Project LE-277, Prog. Rep. No. 5*, 1980.
8 W. Kappus, in preparation.
9 U. Hullmeine, W. Kappus, J. Schulz, E. Voss and A. Winsel, *ILZRO Project LE-277, Prog. Rep. No. 4*, 1979.
10 A. Winsel, H. Laig-Hoerstebrock, K. Ledjeff, H. Tochtermann and R. Schneider, *Final Rep. US-DOE Contract 31-109-38-4438*, 1979.
11 A. Winsel, unpublished results, 1977.
12 U. Hullmeine and W. Kappus, unpublished, 1979.